Valence-electron distribution in MgB_2 by accurate diffraction measurements and first-principles calculations

Lijun Wu, Yimei Zhu,* T. Vogt, Haibin Su, and J. W. Davenport
Brookhaven National Laboratory, Upton, New York 11973, USA

J. Tafto
University of Oslo, P.O. Box 1048, Blindern, 0316 Oslo, Norway

(Received 7 March 2003; revised manuscript received 24 September 2003; published 3 February 2004)

We use synchrotron x-ray and precision electron-diffraction techniques to determine accurately the structure factors of reflections that are sensitive to the valence-electron distribution in the superconductor MgB_2. These values deviate significantly from those calculated using the scattering factors of free (or neutral) atoms, but agree well with our calculated structure factors based on density-functional theory. Having experimentally established the reliability of our first-principles-based structure factors, we present electron-density maps of the redistribution of the valence electrons that takes place when hypothetical free atoms of Mg and B in MgB_2 interact to form the real crystal.

DOI: 10.1103/PhysRevB.69.064501 PACS number(s): 74.25.Jb, 61.10.−i, 61.14.−x

I. INTRODUCTION

The electronic structure of MgB_2 has received much attention since the discovery of its superconductivity at an astonishing high temperature of 39 K.[1] This material is bound to be a model system in efforts to understand superconducting properties from microscopic first-principles calculations. This is based on the fact that this remarkable material is structurally simple containing only low-Z elements in a small crystal unit cell with high symmetry, $P6/mmm$. It is important to recognize that Mg ($Z=12$) and B ($Z=5$) are light elements and therefore charge transfers lead to relatively large changes in the total charge density compared to free, or neutral, atoms. In x-ray crystallography, most investigations are based on overlapped spherical atomic charge densities, thus neglecting subtle bonding effects.[2,3] The structural simplicity of MgB_2 leads to the situation that just a few months after the discovery of its superconductivity, many first-principles electronic structure calculations based on density-functional theory, DFT, appeared in the literature.[4–7] Virtually all the first-principles calculations that have been published show the same electronic structure and density of states, and thus also the same spatial distribution of electrons. Experimental techniques to verify the calculated bulk electronic structure calculations are x-ray absorption spectroscopy and electron energy-loss spectroscopy, focusing on the fine structure near the absorption edge, and quantitative diffraction using x-rays or fast electrons. Spectroscopy and diffraction are complementary experimental tools. Diffraction techniques are experimentally more demanding than spectroscopic techniques since extremely accurate diffraction measurements are needed to move beyond determining the positions of the atoms (nuclei) within the crystal unit cell towards addressing the rearrangement of valence electrons caused by bonding between the atoms of the crystal. The interpretation of the spectroscopic data, on the other hand, poses an additional theoretical challenge because the ejection of core electrons forces the system into an excited state while DFT applies strictly only to the ground state. Several studies have recently addressed the electronic structure of MgB_2 using spectroscopic techniques,[8,9] including the anisotropy of the hole states near the Fermi level.[10–12]

In this work, we use a quantitative electron-diffraction technique we have developed recently[13] to accurately measure the structure factors of low-order reflections that are very sensitive to the charge distribution in materials. We also use synchrotron x-ray powder diffraction to measure high-order reflections. DFT calculations of the electronic structure of MgB_2 are then tested by these diffraction measurements in order to study the rearrangement of the electron density as compared to the electron density in a hypothetical crystal with atoms having the electron distribution of free, or neutral, atoms (overlapped spherical atom densities, here termed as procrystal). Using x-ray diffraction we extract structure factors that are the Fourier components of the electron density in the crystal. With electron diffraction we determine the Fourier components of the electrostatic potential. The final step of converting to x-ray structure factors is straightforward for short **g** vectors, while for larger **g** vectors the thermal parameters need to be determined with high accuracy. Likewise the electron density that we calculate by DFT can be represented by its Fourier components.

X-ray and electron diffraction are complementary. X-ray diffraction measures the total density of electrons in crystal; in contrast, electron diffraction measures electrostatic potential, i.e., the total electron density as well the nuclear core charge. With x rays we collect a powder pattern containing many reflections, while with electrons we can determine accurately a few selected structure factors, and due to the small electron probe, a tiny powdered grain or a crystal smaller than 100 nm can be easily studied as a single crystal. Electron diffraction is particularly sensitive to valence-electron distribution in crystals at short reciprocal vectors, and thus the structure factors determined from electron diffraction at small scattering angles give valuable information about electron transfer over longer distances in the crystal unit cell. This becomes evident when considering the Mott-Bethe for-

 ©2004 The American Physical Society

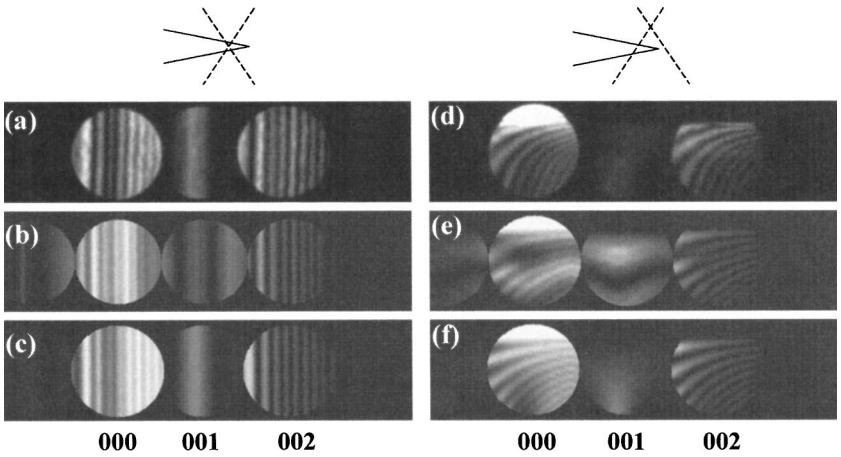

FIG. 1. Conventional convergent beam electron diffraction patterns: (a) experimental (b) calculated for procrystal, and (c) best fit to the experiment. PARODI patterns: (d) experimental, (e) calculated for procrystal, and (f) best fit to the experiment. Sketches of experimental setup for both methods using a wedge sample are included at the top of the figures.

mula: $f^{(e)}(s) \propto (1/s^2)[Z - f^{(x)}(s)]$. Here f with superindices e and x refers to the atomic scattering amplitude for electrons and x-ray diffraction, respectively, Z is the charge of the nucleus, and s is the scattering vector. For small s, where $f^{(x)}$ approaches the number of electrons at the atom that is close to Z, the electron-scattering amplitude will vary greatly with the distribution of valence electrons around the atom. This means that the electron diffraction is more suitable for the accurate measurement of the innermost reflections than x-ray diffraction. Measuring accurately just a few of the low-order electron structure factors provides a useful test of electronic structure calculations of the electron density. Electron-density maps of MgB_2 have been published based on electronic structure calculations and on synchrotron x-ray diffraction on powder[14] and single-crystal measurements,[15] but the single crystals grown so far are reported to be off stoichiometry.[15] Neither measurement of electron diffraction nor quantitative comparisons have been made between experiments and the electron density obtained from the first-principles calculations. The objective of this paper is to report such measurements and comparisons that are best done in reciprocal space relying on structure factors.

II. EXPERIMENT AND CALCULATION

The diffraction experiments were done at room temperature using a well-characterized powder of MgB_2.[16] In the electron-diffraction experiments, we focused the electron probe within the individual micrometer sized crystal grains. We operated our 3000F JEOL transmission electron microscope that is equipped with a field-emission gun and a Gatan energy filter, at the accelerating voltage of 300 keV which corresponds to an electron wavelength of 1.97 pm. We use convergent beam electron diffraction to accurately determine the electron structure factors of selected reflections. The conventional way of recording a convergent beam electron-diffraction pattern is to focus the fast electrons on the specimen,[17] resulting in recording the diffraction pattern at a constant thickness, but over the range of incident beam directions defined by the convergent beam angle. We refer to this procedure as conventional convergent beam electron diffraction (CCBED). An experimental energy-filtered CCBED pattern of MgB_2 with the 001 reflection near the Bragg position is shown in Fig. 1(a). A more robust experimental procedure is to focus the electron probe of diameter down to 1 nm some 100 μm above the specimen.[13] Each convergent beam disk will now be a shadow image of the specimen, and we achieve parallel recording of dark-field images, PARODI. An area of diameter of the order 1 μm, depending on the convergent beam angle and the distance from the crossover to the specimen, can be illuminated with electrons. If the specimen varies in thickness over the illuminated area, we thus record the diffraction intensities as a function of thickness in addition to the incident beam direction. When compared to CCBED, PARODI adds a new dimension, namely, the thickness, to the experiment, as shown in Fig. 1(d), thus providing additional information in each diffraction disk which is extremely sensitive to small changes of the crystal and electronic structure under investigation. In this study we excluded the inelastically scattered electrons from the diffraction patterns using an energy filter with an energy window of 5 eV.

To extract structure factors from CCBED as well as PARODI patterns, we perform dynamical Bloch wave calculations of the diffraction intensities as a function of thickness and crystallographic direction of the incident beam. For MgB_2 we know the crystal structure and start by using structure factors of the procrystal, i.e., based on the scattering factors of free atoms. These scattering factors are available in the literature based on Dirac-Fock calculations.[18] Then iteratively we change the structure factors until we arrive at the best agreement with experiment.

To study reflections further out in reciprocal space we did x-ray powder-diffraction measurements on beam line X7A at the National Synchrotron Light Source (NSLS) at BNL using x rays of wavelength 79.991 pm. The sample was contained in a 0.2-mm capillary which was spinning during the measurement at a speed of about 1 Hz to eliminate preferred

TABLE I. Experimental structure factors of the four innermost reflections of MgB_2 from electron diffraction and compared with those calculated for free atoms (the hypothetical procrystal) at $T=298$ K.

Reflection	Observations	Procrystal
001	-0.20 ± 0.03	-0.91
100	0.94 ± 0.05	0.63
101	2.60 ± 0.06	2.69
002	2.93 ± 0.05	2.94

orientation. The data were refined using the Rietveld analysis program PROFIL.

First-principles calculations of the electron density and structure factors for both low-order and high-order reflections were carried out using DFT. The DFT equations were solved using the full potential linear augmented plane-wave method, FLAPW, as embodied in the WIEN code.[19] For the exchange-correlation potential we used the generalized gradient approximation of Perdew.[20]

III. RESULTS AND DISCUSSIONS

Figures 1(b,c) and 1(e,f) show calculated CCBED and PARODI patterns, respectively. In these calculations we used the room-temperature lattice parameters determined by Vogt *et al.*[16] with $a=0.3086$ nm and $c=0.3521$ nm, and the Debye-Waller factor $B=0.4$ for both boron and magnesium.[21] We start from the structure factors of free atoms to match calculations with experiments as shown in Figs. 1(a) and 1(d). The best fit using CCBED as well as PARODI resulted in an electron structure factor $F_{001}=-0.20$ Å [Figs. 1(c) and 1(f)] as compared to -0.91 Å [Figs. 1(b) and 1(e)] for the procrystal. We did similar experiments and fitting for the 100, 101, and 002 reflections. The measured structure factors for the four reflections together with those calculated for the procrystal are shown in Table I. Increased deviations between the experiments and the procrystal model are noticed with the decrease of length of the reciprocal vectors, suggesting the high sensitivity to the crystal ionicity at small scattering angles. The electron structure factors were converted to the x-ray structure factors based on the following relationship:

$$F_g^x=\left[\sum_i Z_i \exp\left(-B\frac{g^2}{4}\right)\exp\left(-2\pi i g\cdot r\right)\right]-\left(C\frac{g^2}{4}F_g\right).$$

Here B is the Debye-Waller factor, $C=8\pi\varepsilon_0 h^2/m_e e^2=41.78$ when the electron structure factor F_g and the reciprocal-lattice vector g are given in angstrom and reciprocal angstrom units, respectively. The experimentally measured x-ray structure factors and those converted from electron structure factors and calculations based on DFT and procrystal are listed in Table II. In Table II, we note much smaller measurement error for the 001 and 100 structure factors converted from the electron diffraction than from the direct x-ray measurements. This is typical for reflections at small scattering angles. The reason is that the incident fast electrons interact with the electrostatic potential that includes the contribution from the positive charge at the nucleus. This results in large changes in the electron-scattering amplitudes of the atoms at low scattering angles when valence electrons are redistributed. This confirms experimentally, as argued in the Introduction, that electron structure factors for short reciprocal vectors are highly sensitive to charge transfer. We have previously shown that this is the case for the high-temperature oxide superconductors[13] that have large c axes and thus some reciprocal vectors are much shorter than the shortest found in MgB_2.

In the DFT calculations, the lattice parameters corresponding to a minimum in the energy were $a=0.3081$ nm and $c=0.3528$ nm in good agreement with experiment and other DFT calculations. The band structure and density of states were also in good agreement with previous work.[4–7] We note that the WIEN code is a full potential implementation of the density-functional equations. So, for example, the charge density is not constrained to be the overlap of spherical charge densities but rather contains whatever nonspherical contributions are allowed by the crystal symmetry. Further, the charge density is determined self-consistently and bears no particular relation to overlapped atomic densities. Previous calculations for diamond, silicon, and germanium[3] show that well-converged, full potential, DFT results such as those reported here agree with experimental structure factors to better than 1%.

The main purpose of the synchrotron x-ray experiments was to measure the structure factors of high-order reflections. Figure 2(a) shows the x-ray powder diffraction of MgB_2. The structure factors, obtained from the measured intensities, are listed in Tables II and III, respectively. In Table III we compare the experimentally determined structure factors with those calculated using DFT and those calculated for the procrystal. We note that the R factor between the measure-

TABLE II. X-ray structure factors of the four innermost reflections of MgB_2 at $T=298$ K and also those converted from experimental electron diffraction compared with calculations.

	Observations		Calculations	
Reflection	X-ray diffraction	Converted from electron diffraction	DFT	Procrystal
001	1.96 ± 0.51	2.15 ± 0.03	2.18	2.75
100	5.91 ± 0.17	5.53 ± 0.07	5.70	5.98
101	11.82 ± 0.08	10.64 ± 0.14	10.45	10.42
002	11.80 ± 0.08	11.43 ± 0.17	11.41	11.40

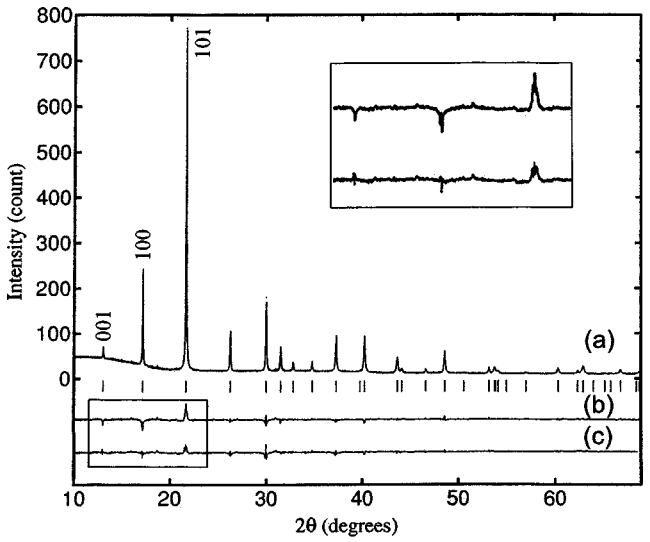

FIG. 2. Fitting results of Rietveld analysis of MgB_2 x-ray powder diffraction. (a) Experimental observation, (b) difference spectrum refined as MgB_2 with $R_{wp}=11.2\%$ and $R_1=11.5\%$ where $R_{wp}=\sqrt{\Sigma w(I'_{obs}-I'_{cal})^2/\Sigma w I'^2_{obs}}$ and $R_1=\Sigma(I_{obs}-I_{cal})/\Sigma I_{obs}$, and (c) difference spectrum refined as MgBC with $R_{wp}=9.7\%$ and $R_1=8.3\%$. Insets are the enlarged box area (001, 100, and 101 reflections) in (b)(c).

ment and DFT defined as $R=\Sigma_g|F_{obs}-F_{dft}|/\Sigma_g F_{dft}$, is similar to the R factor between the measurement and the procrystal since the reflections further out in reciprocal space are not sensitive to the charge transfer. Based on these experimental measurements, a structural model was then obtained using a Rietveld refinement procedure. In the initial stage of the refinement and using the scattering factors of free atoms, a rather unsatisfactory fit was achieved as seen in the difference pattern in Fig. 2(b). Subsequent refinements using the scattering factor of Mg^{2+} resulted in a significant improvement. The refinements were further improved when using a Mg^{2+} form factor and simultaneously allowing the occupancy of boron to refine to a value above full occupancy $n_B=2.3(1)$. This suggests that a significant amount of negative charge is transferred to the boron layer. Two different atomic species, boron and carbon, were located on the boron site to simulate the fact that B^- $(2s^2\,2p^2)\equiv C$ since the scattering factor of B^- is unavailable in literature. Their occupancies $n_B=1.06(6)$ and $n_C=0.94(6)$ indicate that roughly one extra electron is required in the boron site to achieve a good fit of the data [see Fig. 2(c)]. The anisotropic displacement parameters of both B and C species were constrained to be the same and are very reasonable and comparable to single-crystal x-ray diffraction studies.[15] We note that in

TABLE III. Structure factors of high-order reflections in MgB_2 at $T=298$ K, compared with those from DFT calculations and the procrystal.

Reflection			Observations	DFT	Procrystal
1	1	0	10.90±0.09	10.22	10.46
1	0	2	5.05±0.20	4.77	4.89
1	1	1	3.06±0.33	3.06	3.04
2	0	0	4.63±0.22	4.62	4.52
2	0	1	7.38±0.14	7.18	7.38
0	0	3	2.12±0.47	2.25	2.42
1	1	2	8.63±0.12	8.34	8.42
1	0	3	6.44±0.16	6.35	6.41
2	0	2	3.34±0.30	3.44	3.47
2	1	0	3.09±0.32	3.14	3.22
2	1	1	5.78±0.17	5.65	5.74
1	1	3	0.94±1.06	1.44	1.51
3	0	0	6.37±0.16	6.31	6.45
2	0	3	4.94±0.20	5.00	5.10
0	0	4	5.90±0.17	6.29	6.36
2	1	2	2.46±0.41	2.46	2.53
3	0	1	0.40±2.52	1.19	1.22
1	0	4	1.68±0.60	2.24	2.32
3	0	2	5.19±0.19	5.47	5.59
2	2	0	5.59±0.18	5.24	5.37
2	1	3	3.94±0.25	4.10	4.19
1	1	4	4.73±0.21	5.20	5.30
3	1	0	1.15±0.87	1.78	1.81
3	1	1	3.43±0.29	3.76	3.85
3	0	3	0.36±2.80	0.59	0.60
2	2	2	3.76±0.27	4.62	4.73

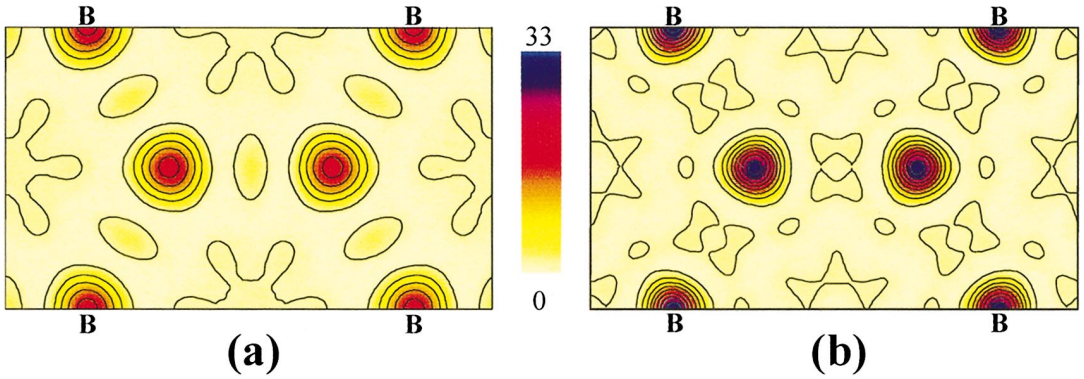

FIG. 3. (Color) DFT calculation of the total electron-density map of the (001) B plane in MgB_2, using (a) 30 reflections and (b) 70 reflections.

x-ray refinements too much electron density in the B layer can be compensated for by introducing Mg deficiency, thus creating an artifact due to using the wrong scattering factors and not necessarily an indication of nonstoichiometry. Thus, reports about nonstoichiometry of MgB_2 based on diffraction alone should be viewed critically.

Our structure factors were measured at room temperature ($T=298$ K), while those calculated using DFT are at $T=0$ K. For comparison, the calculated structure factors were adjusted to room temperature by multiplying a temperature factor $\exp(-Bs^2)$ (we use the same Debye-Waller factor $B=0.4$ (Ref. 21) as in our electron-diffraction refinement). Note that the experimental structure factors are much closer to the self-consistent DFT results than those calculated assuming free atoms. We see, by comparing structure factors, also consistent with the x-ray refinement, that there is charge transfer away from the Mg plane towards the B plane in that there is a significant reduction of the 001 experimental structure factor relative to the one for the procrystal. The 002 structure factor is virtually the same for the electron-diffraction experiments and for the procrystal, suggestive of the fact that charge has moved the whole way from the Mg plane to the B plane.

Figure 3(a) shows the calculated total electron-density

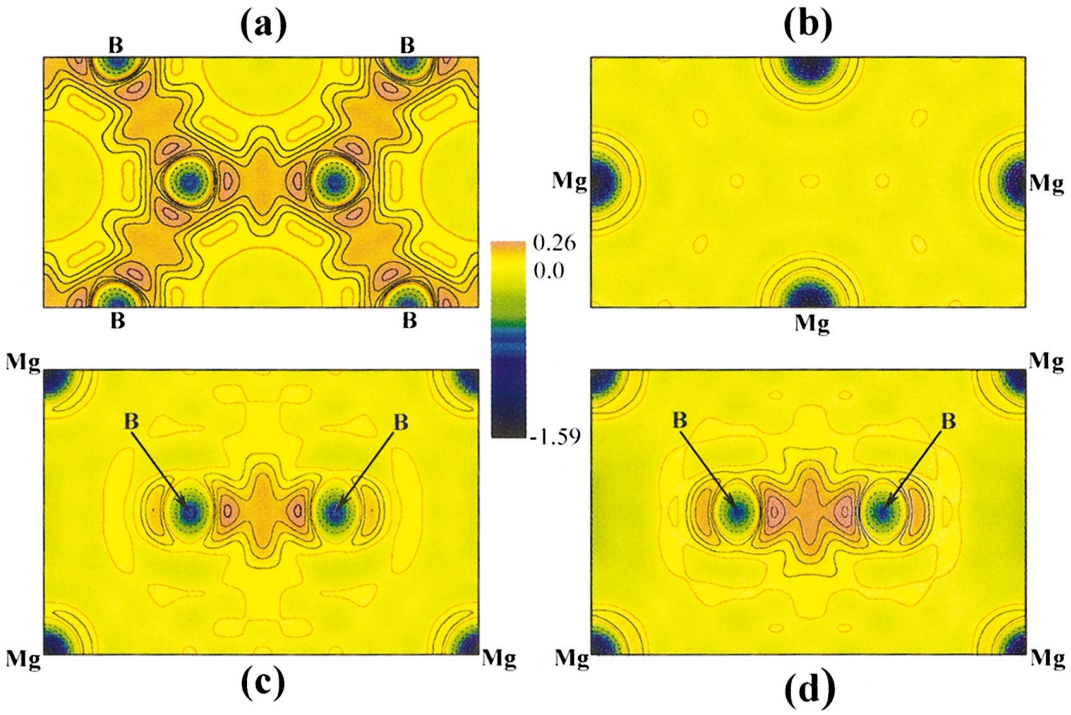

FIG. 4. (Color) DFT calculated difference charge-density maps $\Delta\rho(\mathbf{r})$ with contours shown as dashed black line for $\Delta\rho<0$ with intervals of 0.2 $e/\text{Å}^3$, orange line for $\Delta\rho=0$, and solid black line for $\Delta\rho>0$ with intervals of 0.05 $e/\text{Å}^3$. A color scheme of black-blue-green below zero level, yellow-purple at and above zero level was used. (a) and (b) Planes normal to the c axis through the B and Mg atoms, respectively. (c) The 110 plane through the Mg and B atoms. (d) Differs from (c) in that we have replaced the 001, 100, 101, and 002 DFT calculated structure factors with these four determined by electron diffraction.

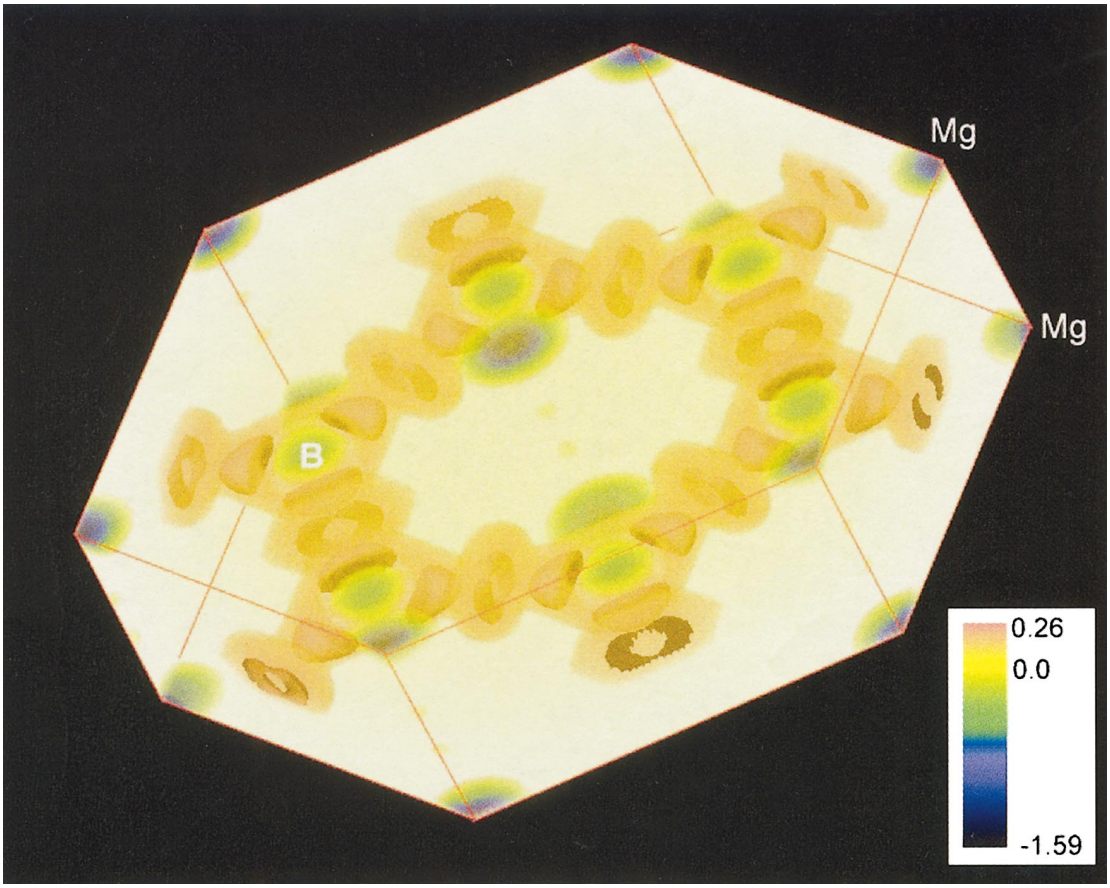

FIG. 5. (Color) A three-dimensional valence-electron distribution in MgB_2 based on precision electron-diffraction measurements and DFT calculations. The map was made with the same color scheme used in Fig. 4. A translucency factor for $\Delta\rho$ around zero $(-0.1–0.1)$ was used to improve the visibility.

map with DFT using 30 reflections, which corresponds to 340 reflections when the multiplicity of the crystal symmetry is considered. The experimental map, obtained using the four low-order reflections from electron diffraction and higher-order reflections from x rays (Table 3), and even the map based on the structure factor calculations for the procrystal exhibited no significant difference. This is expected since the truncation error is unavoidable in a presentation of the total electron-density map due to a limited number of reflections as shown in Fig. 3(b) for 70 reflections. However, in the difference map, which we now will present, the truncation problem is greatly reduced. The reason is that the inaccessible structure factors far out in reciprocal space would mainly contribute to reducing the spatial resolution in the difference map.

In order to make a quantitative comparison with experiments and other calculations we first synthesized the difference density (called the static deformation density in Ref. 3) from the calculated DFT structure factors and those of the procrystal,

$$\Delta\rho(\mathbf{r}) = \rho(\mathbf{r})_{\mathrm{DFT}} - \rho(\mathbf{r})_{\mathrm{PRO}} = \frac{I}{V}\sum_{g} (F_{g_{\mathrm{DFT}}} - F_{g_{\mathrm{PRO}}}) \exp(-2\pi i \mathbf{g}\cdot\mathbf{r}),$$

where the sum was carried out for $|\mathbf{g}| \leqslant 2\ \text{Å}^{-1}$, which corresponds to nearly 1000 reflections with ~70 being independent. In Fig. 4 we present the difference electron-density maps through different planes in real space. Figures 4(a) and 4(b) show cuts normal to the *c* axis through the B planes and Mg planes, respectively. Figure 4(c) shows the difference map through the atoms in the 110 plane containing both Mg and B atoms, and Fig. 4(d) a similar map after replacing the 001, 100, 101, and 002 structure factors in the DFT calculations with those determined by electron diffraction. We note that the difference charge density in the B plane [Fig. 4(a)] is remarkably similar to the valence-charge density in the (0001) plane of graphite.[22,23] In this work we want to provide robust tests for the DFT calculations by keeping the number of adjustable parameters to a minimum. Apart from the structure factors that we are aiming at, the only adjustable parameter using CCBED is the crystal thickness at the area we focus the electron probe, and in PARODI the angle of the crystal wedge. The structure factors that are most reliably tested experimentally are the innermost since they are negligibly influenced by thermal parameters. These are the structure factors that we can determine with high accuracy using quantitative electron diffraction. This is seen in Table I where we note that the experimental electron structure factor of the 001 reflection is only 20% of that for the procrystal, i.e., the

hypothetical crystal with no rearrangement of the valence electrons. The similar percentage for the 100 reflection is 70%. However, for the majority of the reflections further out in reciprocal space, these deviations typically range between 98% and 102% as they do for the x-ray structure factors based on comparison between DFT and the procrystal calculations. With the electron-diffraction techniques we use here we measure the structure factors on an absolute scale, and are able to assess the accuracy of the fit by doing dynamical calculations with different values of the structure factors.

The four structure factors we have determined experimentally are in reasonable agreement with first-principles DFT calculations, and the 001 structure factor that we have measured precisely using electron diffraction is in excellent agreement with these calculations suggesting that the DFT calculations we performed are adequate in addressing the redistribution of the valence electrons.

It is far from trivial to assign ionic charges to atoms from charge-density maps. The major reason is the overlap between electrons that are attributed to the different ions in a crystal. A way of assigning the charge is to look at the magnitudes of the structure factors. The observation using electron diffraction that the 001 structure factor is 0.60 less than that calculated for the procrystal, Table I, is consistent with two electrons from each Mg atom having moved to the B plane: The x-ray scattering factor of Mg^{2+} is 0.30 less than that of a free Mg atom,[17] and when these electrons move to the boron plane they scatter π out of phase with the Mg ions, resulting in a total reduction of the 001 structure factor of 0.60 relative to the procrystal. On this crucial point our study does not agree with the previous study using the maximum entropy method, reporting that only half of the electrons that leave the Mg atoms move to the B layer at 15 K and none of them at room temperature.[14]

In Fig. 5 we present a three-dimensional electron-density map of the redistribution of the valence electrons in MgB_2, defined as the self-consistent density minus the one obtained from overlapping spherical atomic densities based on the DFT calculations with structure factors up to $\sin\theta/\lambda = 1$ Å^{-1}. A color scheme of blue-yellow-purple was used to represent charge depletion and excess of charge. The characteristic buildup of bond charge between the B atoms is clearly apparent and this charge comes from the Mg as well as the B atoms.

As confirmed by our experimentally tested DFT calculations, electrons are drained away from the Mg atoms and injected into the B plane where virtually the whole excess charge is confined, resulting in Coulomb attraction along the *c* axis, i.e., between the Mg and the B layer. After redistribution the charge in the boron plane is piledup in between the boron atoms, making the boron planes, which are believed to be responsible for the superconductivity, covalent. It is interesting to note that there is also a depletion of charge out to a distance of some 0.05 nm away from the B atoms (a similar charge deficiency was also observed for Mg atoms as indicated in dark blue in Fig. 5). Thus electrons from the Mg as well as the B atoms participate in forming the covalent bonding in the boron plane. Qualitatively, our results agree with other experimental and theoretical studies, but comparisons of the subtle details are not feasible because structure factor values have not been published, and we are aware of only one work that presents difference maps, the x-ray study on single crystals that were reported to be 4.5% lower in Mg.[15] We refer to our prior arguments why this should be viewed with caution when based solely on diffraction experiments. Total electron-density maps are less informative, and probably less reliable without having determined the structure factors extremely far out in reciprocal space due to the truncation errors. Comparison of total electron-density maps from Fourier transform based on our structure factors from DFT and the procrystal by using structure factors reaching out to the interplanar spacing of 0.05 nm showed that the fine details were very similar, signaling that the truncation error, rather than the electron density, is responsible for these fine details [Figs. 3(a,b)]. The truncation problem is virtually absent in the difference map in that there is typically only 2% difference between the structure factors calculated based on DFT and the procrystal model. There are also similarities between our electron-density map and previous x-ray studies,[15] in particular the excess charge in between the B atoms, mainly associated with the σ bonding electrons that have radial symmetry around the line joining neighboring B atoms. A small deviation from radial symmetry, attributed to the π nonbonding electrons, is perceived by comparing Figs. 4(a) and 4(c).

IV. CONCLUSIONS

To summarize, we have studied the valence-electron distribution in the superconductor MgB_2 by accurately measuring structure factors that are highly sensitive to the rearrangement of charge using electron and synchrotron x-ray powder-diffraction techniques and first-principles calculations. Our coordinated experimental and theoretical study show that each Mg atom has donated two electrons to the boron layer, suggesting that the boron layer, in addition to having the same honeycomb structure as the carbon layers in graphite, also has the same number of valence electrons, and these electrons are mainly located in the $p_x p_y$ orbitals between neighboring boron atoms.

ACKNOWLEDGMENT

This work was supported by Division of Materials Sciences, Office of Basic Energy Science, U.S. Department of Energy, under Contract No. DE-AC02-98CH10886.

*Author to whom correspondence should be addressed. Email: zhu@bnl.gov

[1] J. Nagamatsu, N. Nakagawa, T. Muranaka, Y. Zenitani, and J. Akimitsu, Nature (London) **410**, 63 (2001).

[2] P. Coppens, *X-ray Charge Densities and Chemical Bonding* (Oxford University Press, New York, 1997).

[3] Z. W. Lu, A. Zunger, and M. Deutsch, Phys. Rev. B **47**, 9385 (1993).

[4] J. M. An and W. E. Pickett, Phys. Rev. Lett. **86**, 4366 (2001).
[5] K. D. Belashdhenko, M. van Schilfgaarde, and V. P. Antropov, Phys. Rev. B **64**, 092503 (2001).
[6] P. P. Singh, Phys. Rev. Lett. **87**, 087004 (2001).
[7] P. Ravindran, P. Vajeeston, R. Vidya, A. Kjekshus, and H. Fjellvåg, Phys. Rev. B **64**, 224509 (2001).
[8] C. McGuinness, K. E. Smith, S. M. Butorin, J. H. Guo, J. Nordgren, T. Vogt, G. Schneider, J. Reilly, J. J. Tu, P. D. Johnson, and D. K. Shuh, Europhys. Lett. **56**, 112 (2001).
[9] T. A. Callcott, L. Lin, G. T. Woods, G. P. Zhang, J. R. Thompson, M. Paranthaman, and D. L. Ederer, Phys. Rev. B **64**, 132504 (2001).
[10] Y. Zhu, A. R. Moodenbaugh, G. Schneider, J. W. Davenport, T. Vogt, Q. Li, G. Gu, D. A. Fischer, and J. Tafto, Phys. Rev. Lett. **88**, 247002 (2002).
[11] R. F. Klie, Y. Zhu, G. Schneider, and J. Tafto, Appl. Phys. Lett. **82**, 4316 (2003).
[12] R. F. Klie, H. Su, Y. Zhu, J. W. Davenport, J. C. Idrobo, N. D. Browning, and P. D. Nellist, Phys. Rev. B **67**, 144508 (2003).
[13] L. Wu, Y. Zhu, and J. Tafto, Phys. Rev. B **59**, 6035 (1999); Phys. Rev. Lett. **85**, 5126 (2000).
[14] E. Nishibori, M. Takata, M. Sakata, H. Tanaka, T. Muranaka, and J. Akimitsu, J. Phys. Soc. Jpn. **70**, 2252 (2001).
[15] H. Mori, S. Lee, A. Yamamoto, S. Tajima, and S. Sato, Phys. Rev. B **65**, 092507 (2002).
[16] T. Vogt, G. Schneider, J. A. Hriljac, G. Yang, and J. S. Abell, Phys. Rev. B **63**, 220505 (2001).
[17] J. M. Zuo, M. Kim, M. O'Keeffe, and J. C. H. Spence, Nature (London) **401**, 49 (1999).
[18] D. Rez, P. Rez, and I. Grant, Acta Crystallogr., Sect. A: Found. Crystallogr. **50**, 481 (1994).
[19] P. Blaha, K. Schwarz, G. Madsen, D. Kvasnicka, and J. Luitz, WIEN2K (Karlheinz Schwarz, Techn. Universitat Wien, Austria, 2001).
[20] J. P. Perdew, J. A. Chevary, S. H. Vosko, K. A. Jackson, M. R. Pederson, D. J. Singh, and C. Fiolhais, Phys. Rev. B **46**, 6671 (1992).
[21] J. D. Jorgensen, D. G. Hinks, and S. Short, Phys. Rev. B **63**, 224522 (2001).
[22] J.-C. Charlier, X. Gonze, and J.-P. Michenaud, Phys. Rev. B **43**, 4579 (1991).
[23] R. Chen, P. Trucano, and R. F. Stewart, Acta Crystallogr., Sect. A: Cryst. Phys., Diffr., Theor. Gen. Crystallogr. **A33**, 823 (1977).